JOURNAL OF MATERIALS SCIENCE 18 (1983) 3011–3022

Electron microscopic investigations on a melt-quenched Al–Rh alloy

ZARIFF A. CHAUDHURY, C. SURYANARAYANA
Centre of Advanced Study in Metallurgy, Department of Metallurgical Engineering, Banaras Hindu University, Varanasi 221 005, India

An Al–2 wt% Rh alloy was subjected to rapid quenching from the molten state and transmission electron microscopy and diffraction techniques were extensively used to characterize the phases present. Melt quenching led to the formation of a homogeneous solid solution, indicating a substantial increase in solid solubility limit over the equilibrium value. Although stable up to about 640 K, the supersaturated solid solution decomposed at elevated temperatures to a mixture of aluminium solid solution and an intermediate phase, which has been identified to have a monoclinic structure with $a = 1.636$ nm, $b = 0.805$ nm, $c = 1.279$ nm and $\beta = 107.77°$ with a stoichiometry corresponding to $Al_{13}Rh_4$. Although heterogeneous nucleation at grain boundaries was the predominant feature, the precipitate also formed as Widmanstätten platelets inside the grains. This phase has been shown to be an equilibrium phase. Very long annealing treatments at temperatures of 773 K resulted in the formation of an ordered phase. The long-range order was destroyed on heating to still higher temperatures. The equilibrium constitution of the alloy has been shown to be a mixture of $Al_{13}Rh_4$ and aluminium solid solution.

1. Introduction

Many novel metastable phases have been produced in alloy systems by employing ultrafast quenching rates to solidify the corresponding melts. These techniques, commonly referred to as splat cooling, melt quenching or liquisol quenching, owe their origin to Duwez [1] and involve cooling rates often exceeding about 10^5 K sec^{-1}. The associated high rate of solidification has been found to result in (a) refinement of grain size, (b) extension of solid solubility limits, (c) production of metastable crystalline intermediate phases, (d) formation of metallic glasses and (e) modification of segregation patterns [2–6].

As part of a continuing programme on the formation and decomposition of metastable phases in alumimium-base alloys, we had undertaken detailed investigations on Al–Pd [7, 8], Al–Ru [9, 10], Al–Zr [11] and Al–Rh [12, 13] systems. These systems helped in delineating some interesting features of decomposition behaviour in the Al–transition metal systems. The present paper reports on a detailed transmission electron microscopic investigation on the morphology, formation and decomposition behaviour of metastable phases produced in an Al–Rh alloy rapidly quenched from the melt.

The room temperature solid solubility of rhodium in aluminium under equilibrium conditions is negligible (< 0.1 at%). A series of intermediate phases with the stoichiometry Al_9Rh_2, Al_5Rh_2, Al_4Rh, $Al_{3+x}Rh$, and AlRh have been reported to form in Al-rich Al–Rh alloys [14–16]. A new equilibrium intermediate phase with the chemical formula $Al_{13}Rh_4$ has been recently reported by us [13].

The metastable behaviour of Al–Rh alloys subjected to rapid quenching from the liquid state has not been studied so far by others. However, we have recently studied vapour-deposited Al–Rh alloys and reported the microstructures and crystal structures of the as-deposited and annealed thin films [12].

2. Experimental procedure

An Al–2 wt% Rh alloy was prepared as described

0022–2461/83 $03.00 + .12

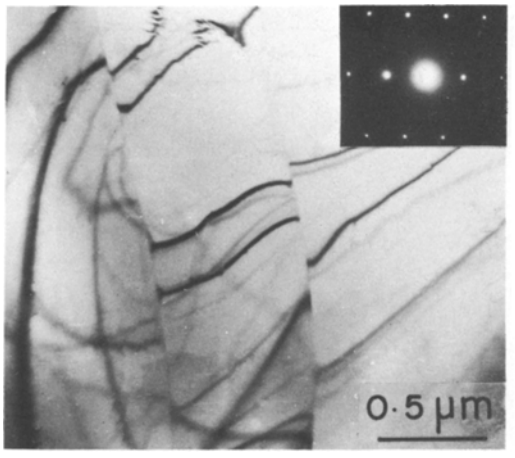

Figure 1 Micrograph showing the formation of elongated grains of aluminium supersaturated solid solution devoid of any precipitation. The diffraction pattern is shown as an inset.

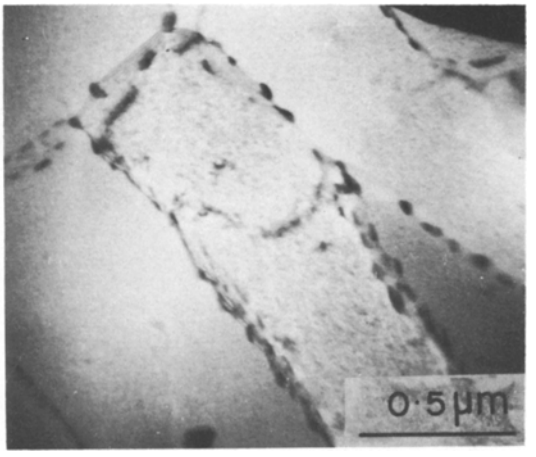

Figure 2 Microstructure showing bimodal distribution of the precipitates. Very fine precipitate in good contrast inside some of the grains and coarse precipitates along the grain boundaries can be seen.

in our earlier paper [12]. Small quantities (about 100 mg) of the alloy were induction melted and rapidly quenched from the liquid state using the conventional "gun" technique [17]. The cooling rate was estimated to be in the range of 10^5 to 10^8 K sec^{-1} depending on the thickness of the sample and thus it was possible to achieve a variety of microstructures. The resultant foils were thin enough in many areas to be examined directly in a Philips EM 300 transmission electron microscope fitted with a goniometer stage and operating at 100 kV.

In situ hot-stage electron microscopy was carried out on many foils to follow the transformation to the equilibrium phases. In some cases, long annealing treatments were given at high temperatures to samples enclosed in evacuated silica tubes. The as-quenched as well as annealed foils were fully characterized under diffraction and imaging conditions. The crystal structure data of the phases obtained by electron diffraction techniques were also corroborated by X-ray diffraction methods.

3. Results

3.1. As-quenched microstructure

Extended solid solubility of rhodium in aluminium was observed in the as-quenched condition in many electron-transparent areas of the foils. A typical electron micrograph is shown in Fig. 1 featuring elongated grains and devoid of any precipitation. The corresponding diffraction pattern, shown as an inset, clearly reveals that this alloy in the as-quenched condition is a homogeneous solid solution.

In relatively thicker foils, where the cooling rate is decidedly lower than in thinner areas, precipitation seems to have taken place (Fig. 2). This micrograph shows a bimodal distribution of the precipitates – a very fine precipitate in good contrast inside some of the grains and relatively coarse precipitates along the grain boundaries. The shape of the grains, however, indicates that perhaps this area also would have originally solidified as a solid solution containing 2 wt% Rh and subsequently precipitation would have taken place first heterogeneously (along grain boundaries) and subsequently homogeneously (inside the grains). These observations clearly indicate that the solid solubility of rhodium in aluminium in the melt-quenched condition can be increased at least up to 2 wt%. As mentioned in Section 1, the equilibrium solid solubility of rhodium in aluminium is practically negligible and thus the present result shows a notable increase in the solid solubility limit.

3.1.1. Cellular structures

Cellular structures are generally observed in several melt-quenched aluminium alloys [7, 18]. These structures are commonly characterized by the presence of dark parallel bands in an otherwise featureless area as shown in Figs. 3a and b. In the absence of diffraction evidence for the presence of a second phase, the dark features cannot be considered as a second phase. A high magnification

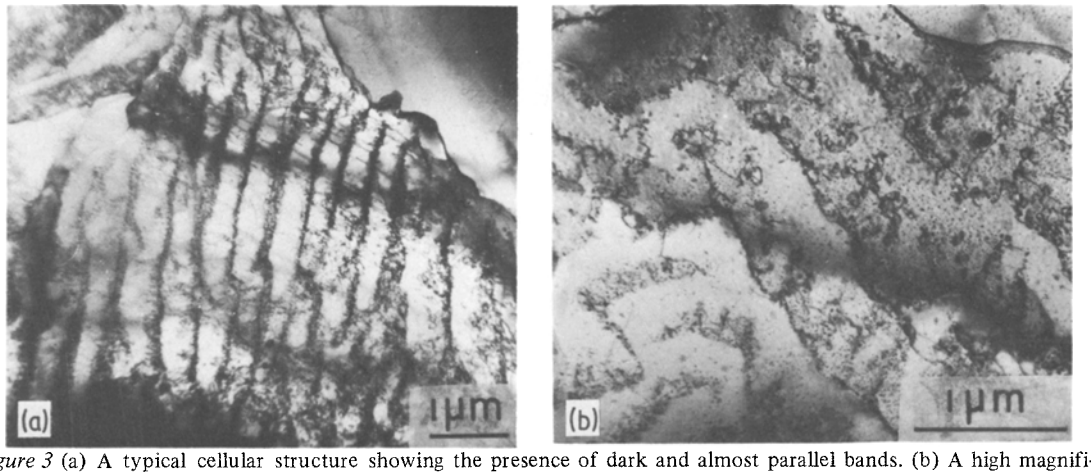

Figure 3 (a) A typical cellular structure showing the presence of dark and almost parallel bands. (b) A high magnification photograph showing that the dark areas comprise perhaps dislocation structures.

photograph (Fig. 3b) shows that the dark areas probably comprise dislocation structures. Thus, it may be very reasonable to consider that these dark bands are due to the bulk slip process as suggested by Williams and Edington [18].

3.1.2. Defect structures

Several types of defect structures were occasionally observed in rapidly quenched alloys, a succinct summary of which was prepared by Jones [19]. Several isolated dislocations (Fig. 4a), sometimes well arranged (Fig. 4b), helical dislocations (Fig. 4c) and some vacancy loop-like structures along with dark bands (Fig. 4d) are some of the features observed in the present investigation. Although, all these defect structures are normally observed in many solid-state quenched materials, observations of these in melt-quenched alloys have been few and far between [7, 20–22]. It is expected that the release of strain energy introduced during solidification is responsible for the defects introduced into rapidly solidified foils. Some of the dislocations could also have formed due to the aggregation of vacancies.

3.2. Decomposition behaviour

With a view to evaluate the stability of the supersaturated solid solution and also to characterize the decomposition products, hot-stage electron microscopy has been performed on these alloys. Fig. 5 shows the sequence of micrographs recorded during continuous heating of a foil from room temperature to about 828 K. (This represents the same area as shown in Fig. 1). Fig. 5a shows the microstructure when the foil was heated up to about 548 K. No clearly visible precipitate is seen in the micrograph, indicating that the supersaturated solid solution is quite stable. Fig. 5b shows the nucleation of the precipitate along the grain boundaries when the foil was heated up to 643 K. On continued heating (Figs. 5c to f), the grain boundary precipitates started growing in size. It is also worth noticing that at a temperature of about 697 K (Fig. 5c) thin platelet-like precipitate started appearing inside the grains, which also continued to grow in length in addition to thickening with temperature. In Figs. 5d to f, precipitation along several grain boundaries can also be noticed. Figs. 6a and b very clearly reveal that these platelets are arranged in a Widmanstätten pattern following specific crystallographic directions. These have been worked out to be $\langle 2\,1\,0 \rangle_{Al}$. Fig. 7 shows the microstructure of a foil annealed at 623 K for about 30 ksec indicating a high density of Widmanstätten type of precipitates. Another feature worth noticing here is that some platelets are thick and very long, whereas most of the others are thin and short. A reason for such a difference could be that nucleation took place at different times resulting in size differences of the platelets. From diffraction evidence, it has been confirmed that both types of precipitates have the same crystal structure.

Further heating, almost up to the melting point of the alloy, results in the slow growth and redissolution of the precipitate (Fig. 8a) and melting of the alloy. However, on cooling from this temperature, a microstructure as shown in Fig. 8b is

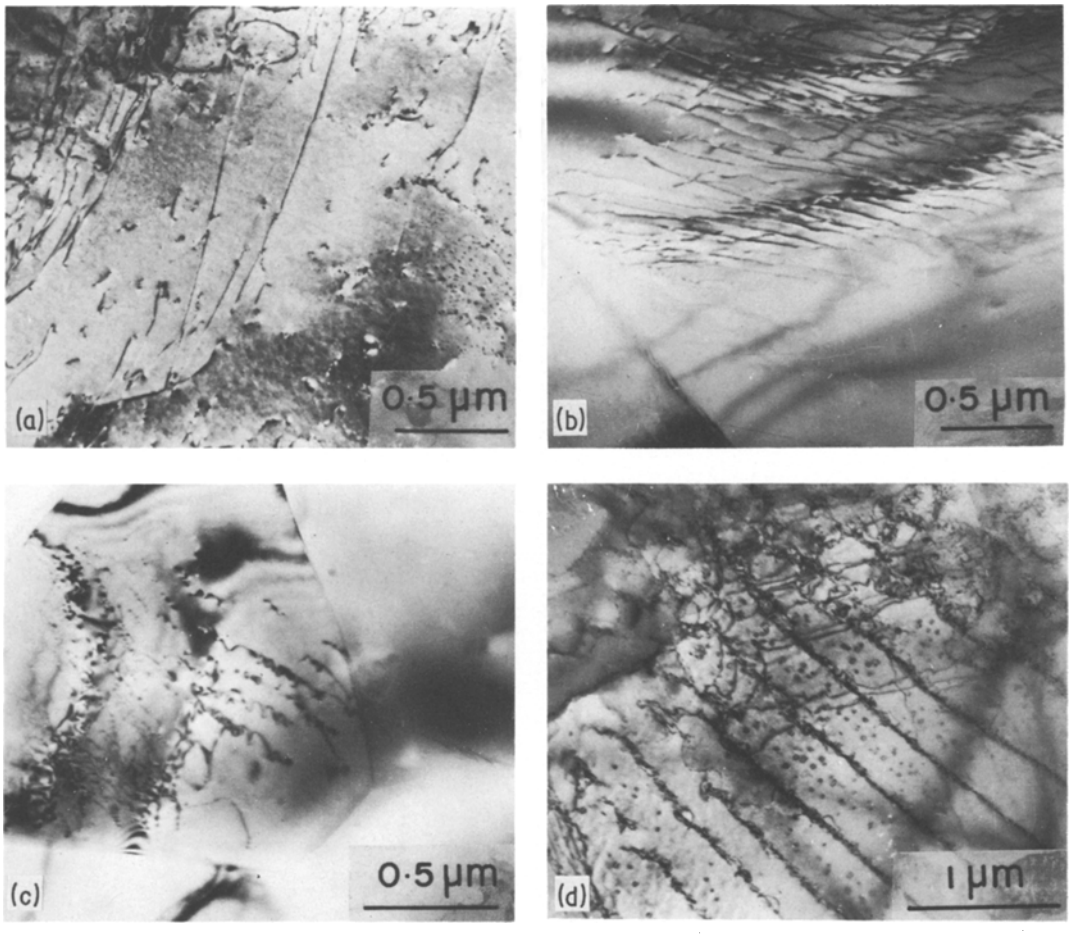

Figure 4 Several types of defect structures observed in the melt-quenched Al–2% Rh alloy. (a) Isolated dislocations, (b) well-arranged dislocations, (c) helical dislocations and (d) vacancy loop-like structures and bands.

obtained. On cooling this alloy to room temperature, a microstructure containing two phases is obtained. Most of the areas show a lamellar structure (Fig. 9). It is worth mentioning here that several steps seem to have formed during the formation of the lamellar structure, which offset the lamellae when they cross the steps. This is more evident in a high magnification photograph (Fig. 10). In some areas one observed a fine striated structure (Fig. 11) which can be either fine scale twinning (as observed in Al–Pd [23] alloys) or stacking faults (as in Ag–Ge [24] alloys). The diffraction pattern clearly shows streaking of the diffraction spots in a direction perpendicular to the long axis of the striations.

Typical diffraction patterns from these two-phase structures are shown in Fig. 12. From these diffraction patterns and several others, it has been possible to show that the precipitate phase has a monoclinic structure with $a = 1.636\,\text{nm}$, $b = 0.805\,\text{nm}$, $c = 1.279\,\text{nm}$ and $\beta = 107.77°$, in conformity with our earlier observation [13]. Single crystal diffraction patterns from the precipitates are shown in Fig. 13. These also confirm the crystal structure and lattice parameters mentioned above.

3.2.1. External heat treatments

In addition to the *in situ* heating sequences described above, some foils have been treated externally for very long times at different temperatures. Although most of the results are similar to those described in the above Section, some subtle differences are noticed (essentially because of long durations of annealing at any temperature) and these are described below:

Precipitation started when the foils were given annealing treatments for 3.6 ksec at 623 K

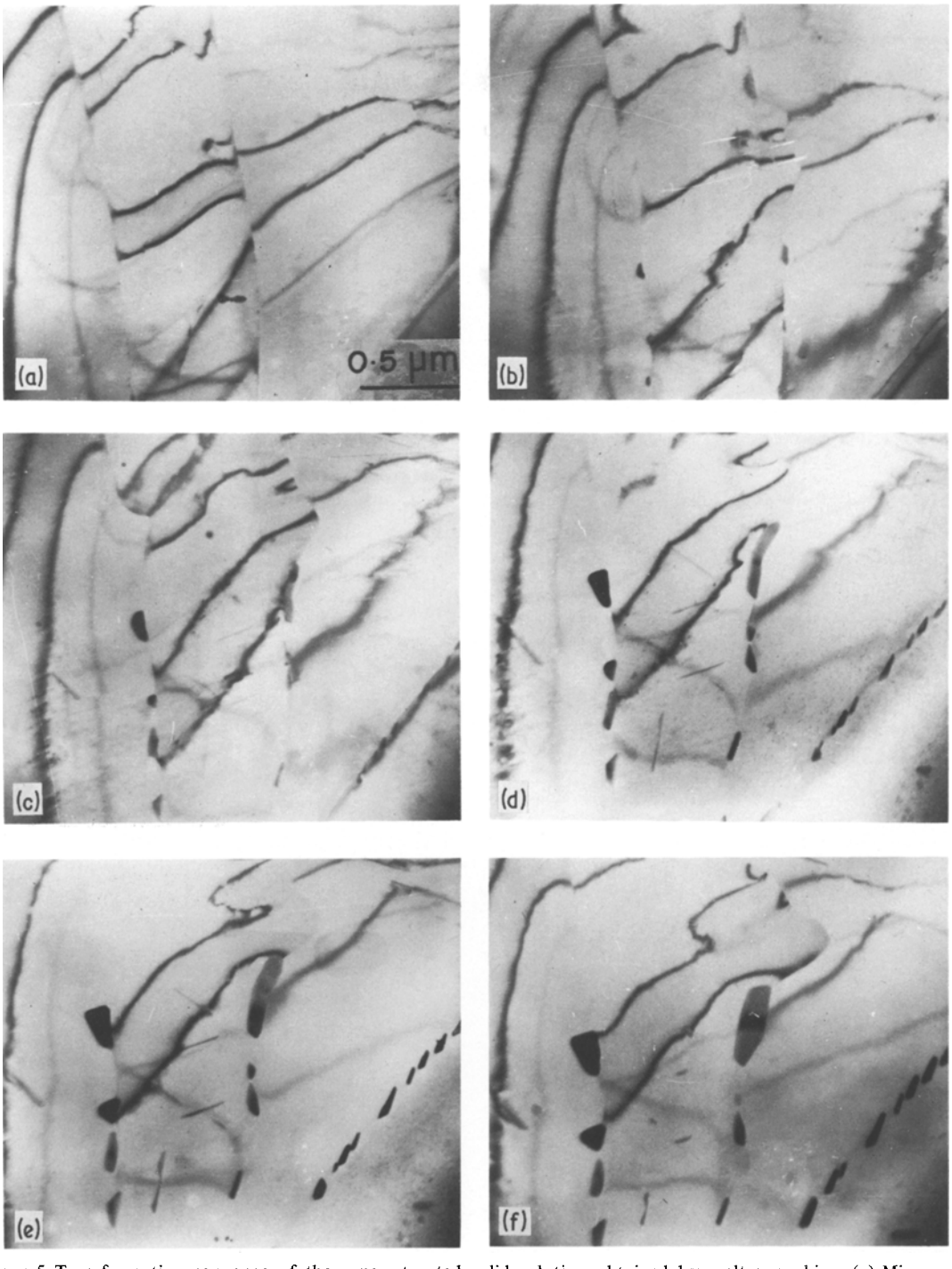

Figure 5 Transformation sequence of the supersaturated solid solution obtained by melt quenching. (a) Micrograph showing absence of precipitation even when heated to a temperature of about 548 K, (b) nucleation of the precipitate along the grain boundaries when heated to 643 K, (c) to (f) show micrographs featuring the growth of grain boundary precipitates on continuous heating. Platelet-like precipitates appear at 697 K (c) and precipitation along several grain boundaries can also be noticed (d and e).

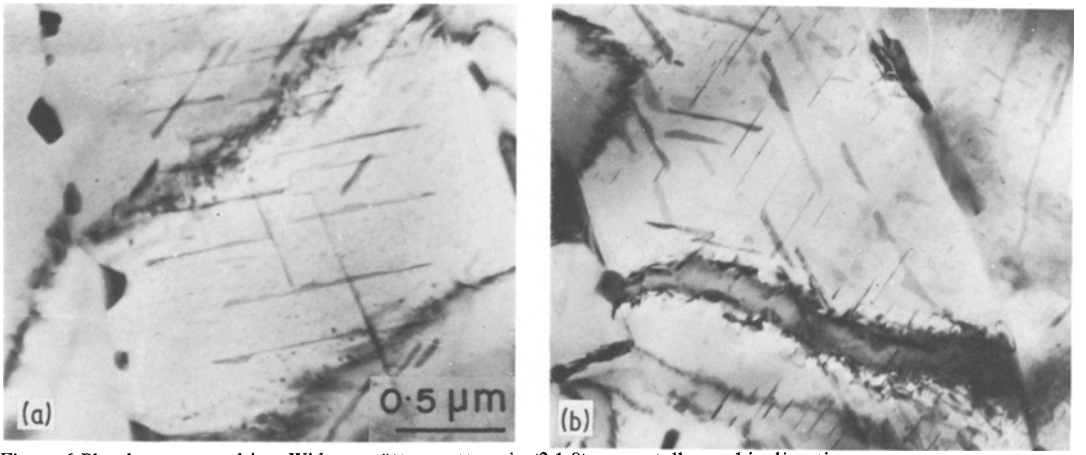

Figure 6 Platelets arranged in a Widmanstätten pattern in $\langle 2\,1\,0 \rangle_{Al}$ crystallographic directions.

(Fig. 14a). Within the grains these seem to be needle-shaped, although bulk-like precipitates are observed along the grain boundaries. Annealing for 11 ksec results in coarsening of the precipitates both along the grain boundaries and within the grains (Fig. 14b). Continued annealing at 773 K for 3.6 ksec results in coarsening of the precipitates further (Figs. 15a and b) and gives rise to diffraction patterns characteristic of the monoclinic structure referred to above.

In addition to the coarsening phenomenon mentioned above, one can also notice, in some areas of the foils, a fine and uniform distribution of precipitates throughout the area (Fig. 16a) when the foils are heat treated at 773 K for about 30 ksec. The diffraction patterns corresponding to this condition are shown in Figs. 16b to d, which clearly indicate the ordered nature of the precipitate. Further, it is interesting to note that the precipitate seems to have a close crystallographic relationship with the aluminium matrix. A strong pointer to indicate that this is an ordered phase is derived from the fact that annealing at higher temperatures (for 30 ksec at 853 K) leads to destruction of long-range order as revealed by streaking observed in the diffraction patterns (Figs. 17a to c).

Figure 7 Micrograph showing a high density of Widmanstätten type of precipitates when the foil is annealed at 623 K for 30 ksec.

4. Discussion

4.1. Supersaturated solid solution

As mentioned above, it has been possible to obtain a completely supersaturated solid solution in the Al–Rh alloy containing 2 wt% Rh. This indicates that melt quenching can increase the solid solubility limit of rhodium in aluminium up to at least 2 wt% Rh. Work with more concentrated alloys can establish the actual metastable solid solubility limit in this system.

Solid solubility extensions by rapid quenching techniques are very common – in fact, this was the first observation made on rapidly quenched foils [25]. Since then, this technique has been routinely employed to achieve supersaturated solid solutions [4], especially in cases where it is impossible to obtain homogeneous solid solutions by solid-state quenching [26]. Solid solubilities of transition metals in aluminium are woefully low under equilibrium conditions, while by rapid quenching from the melt they have been increased by one-to-two orders of magnitude in most of the cases. Thus, rhodium follows the trend of other metals. A detailed discussion in terms of thermo-

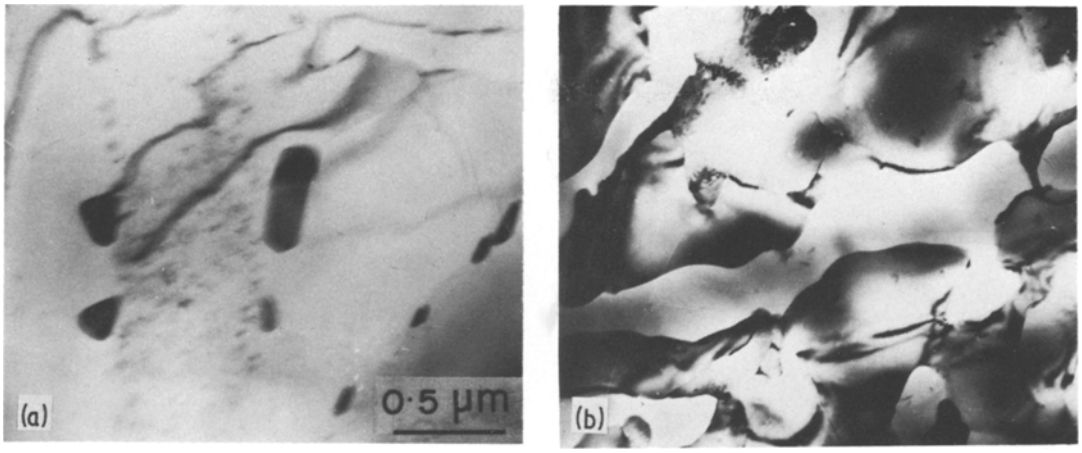

Figure 8 (a) Micrograph showing the redissolution of the precipitates when the foils are heated almost up to the melting point of the alloy. (b) Micrograph showing the features on fast cooling from the temperature obtained in (a).

dynamic parameters on solid solubility extensions is presented in [4] and [27] and will not be repeated here.

4.2. Decomposition behaviour

The as-quenched supersaturated solid solution was quite stable up to 643 K on continued heating, while longer annealing treatments at 573 K also resulted in nucleation of precipitates along the grain boundaries. As was mentioned earlier, there is considerable grain refinement in rapidly quenched alloys and thus heterogeneous nucleation is very easy. This is amply borne out by several experiments in many alloy systems. The same phenomenon is observed in the Al–Rh system as well. Although, the growth and coarsening of the precipitates is of common observation in several alloy systems, a point of interest is that the precipitate seems to take up three different morphologies – fine particles, Widmanstätten platelets and grain boundary idiomorphs. This could be a result of the strong crystallographic orientation relationship between the matrix and the precipitate.

Another point worth noticing in the decomposition process is the formation of a precipitate which has a monoclinic crystal structure and a probable composition of $Al_{13}Rh_4$. More discussion about this will be taken up in the next Section.

When the thin foils have been taken up to almost the melting point of the alloy and suddenly cooled, a lamellar structure is observed indicating that the alloy might have got locally melted and resolidified through a eutectic reaction. The

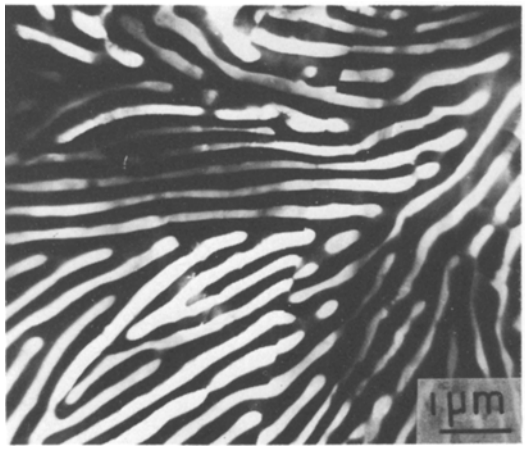

Figure 9 Micrograph showing the two-phase lamellar structure after cooling to room temperature.

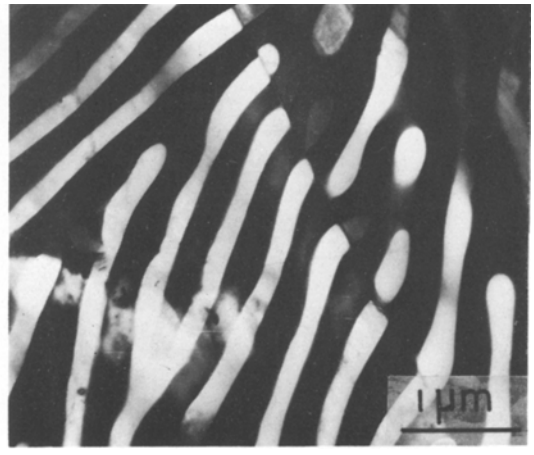

Figure 10 A high magnification micrograph of the lamellar structure showing the offset of lamellae at the steps.

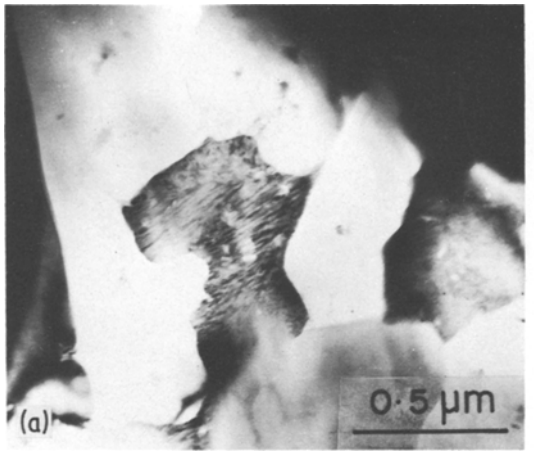

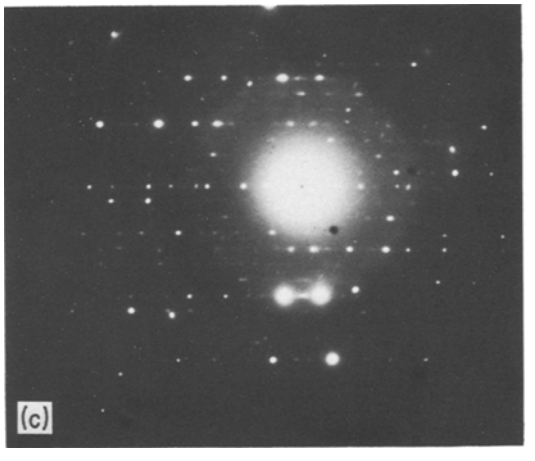

Figure 11 Micrographs showing fine striations indicating the presence of either fine twins or stacking faults: (a) bright-field micrograph, (b) dark-field micrograph, (c) diffraction pattern.

crystal structure of the intermediate phase co-existing with the Al-supersaturated solid solution in the lamellar structure has been found to be monoclinic $Al_{13}Rh_4$. The lamellar structure also shows several steps at which the lamellae are offset. These steps and the striated structure (Fig. 10) could easily result from the strains associated with the rapid cooling of the foil from this high temperature.

Yet another point of interest is the formation of an ordered phase on long annealing (e.g. for 30 ksec at 773 K). The crystal structure of the ordered phase appears to be very complicated. The long-range order was destroyed on heating to a still higher temperature. The streaking associated with the diffraction patterns in Fig. 17 could be due to the transitional short-range order present in the alloy. Further work is required to solve the crystal structure of the ordered phase and the mechanism of disordering.

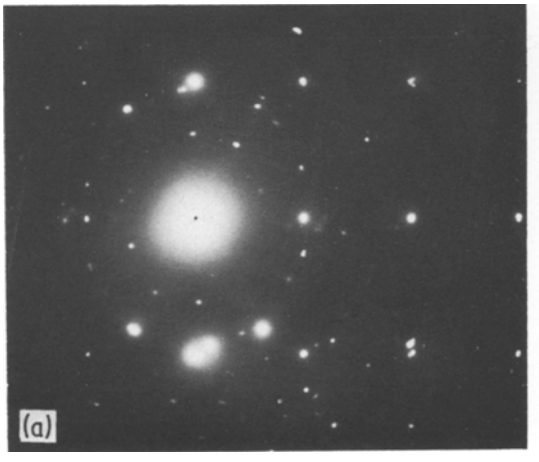

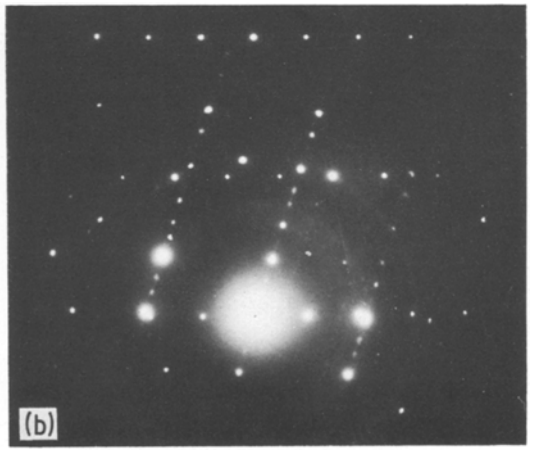

Figure 12 Typical diffraction patterns from the two-phase structures.

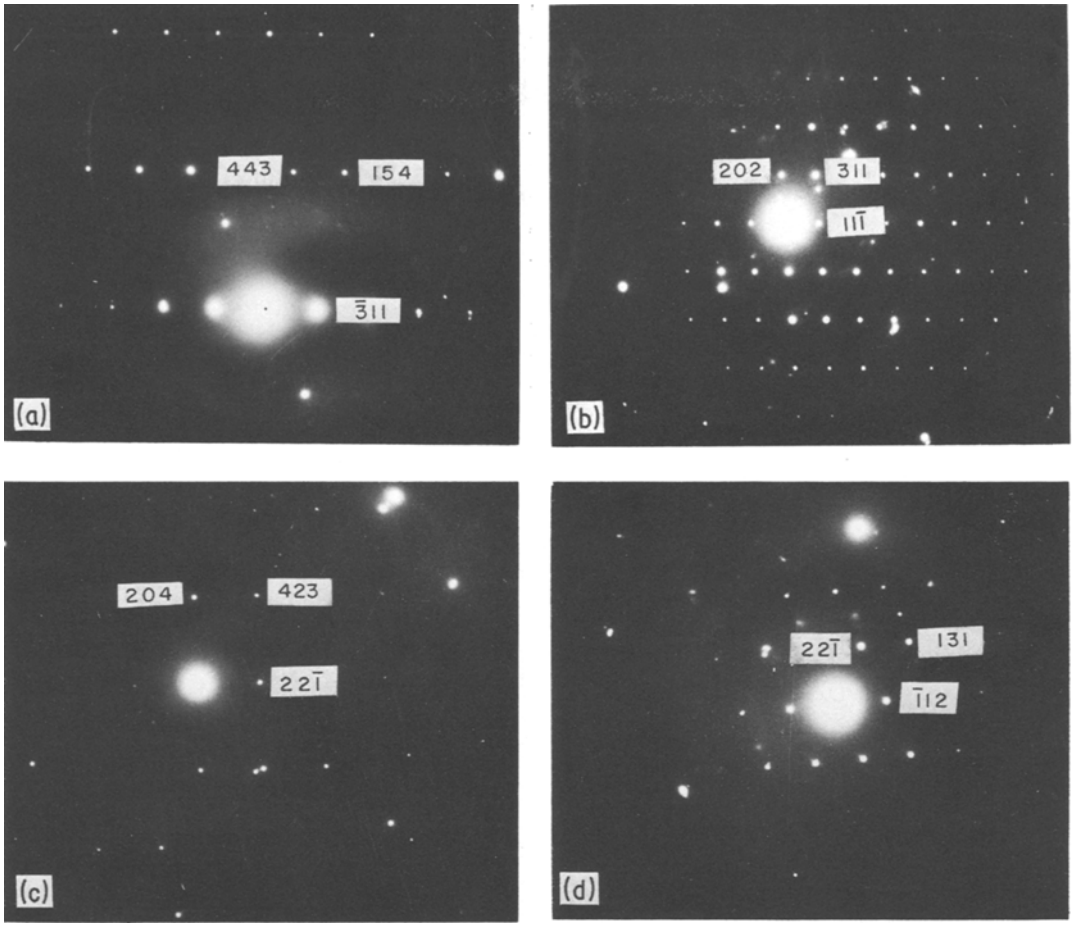

Figure 13 Diffraction patterns from the $Al_{13}Rh_4$ phase. The orientations are (a) $[1\ \bar{1}\bar{3}\ 16]$, (b) $[\bar{1}\ 2\ 1]$, (c) $[\bar{4}\ 5\ 2]$ and (d) $[5\ \bar{3}\ 4]$.

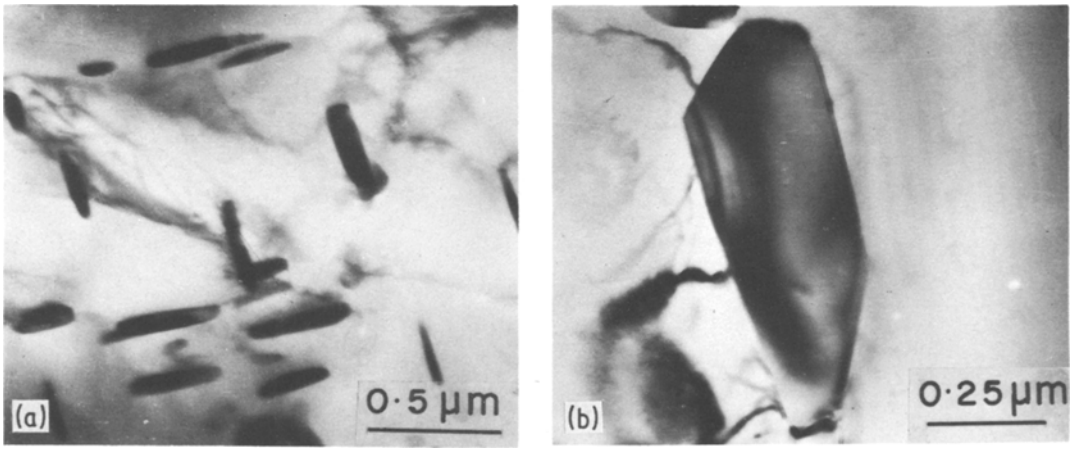

Figure 14 Micrographs showing precipitation when foils are heat treated externally, (a) needle-like precipitates on annealing for 3.6 ksec at 623 K, (b) coarsening of the needles and grain boundary precipitates on annealing for 11 ksec at 623 K.

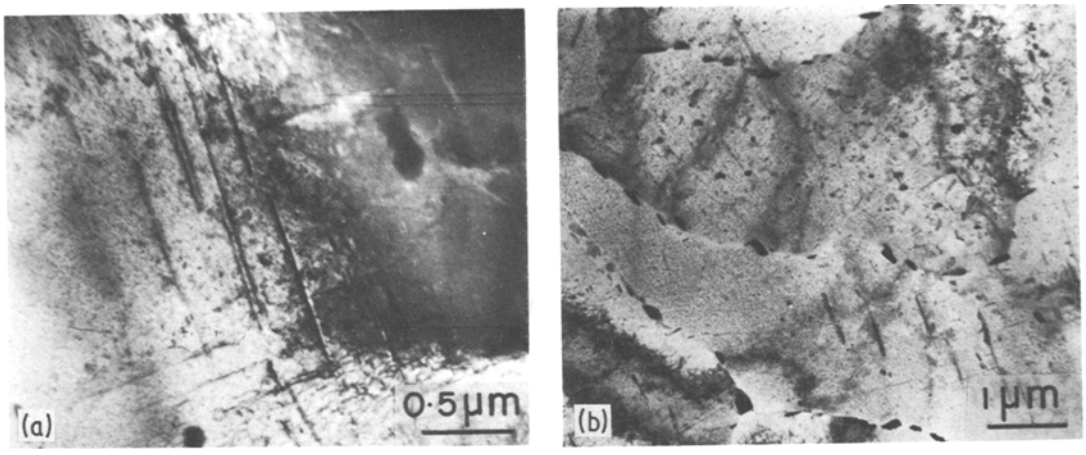

Figure 15 Coarsening of the precipitates on annealing for 3.6 ksec at 773 K, (a) platelets and (b) bulk particles.

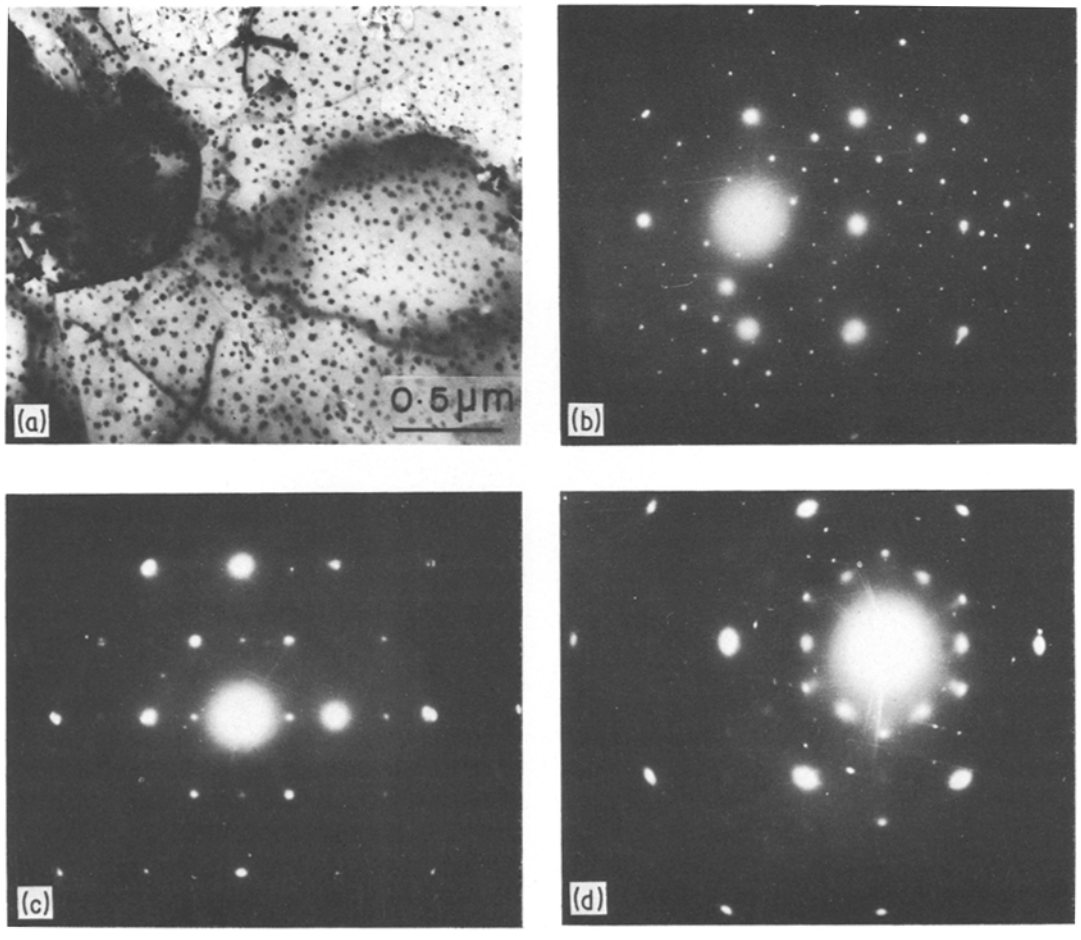

Figure 16 Long annealing for about 30 ksec at 773 K resulted in the precipitation of fine and uniformly distributed precipitates, (a) bright-field micrograph, (b) to (d) typical diffraction patterns indicating that this is an ordered phase.

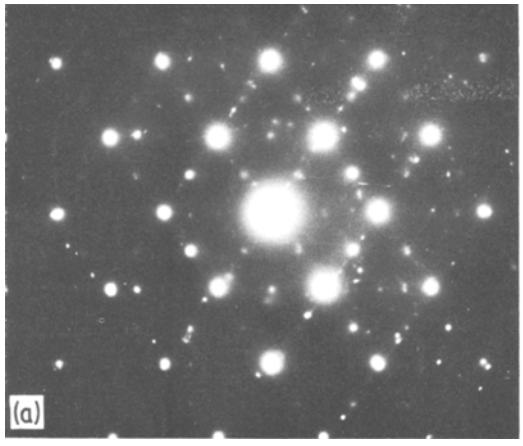

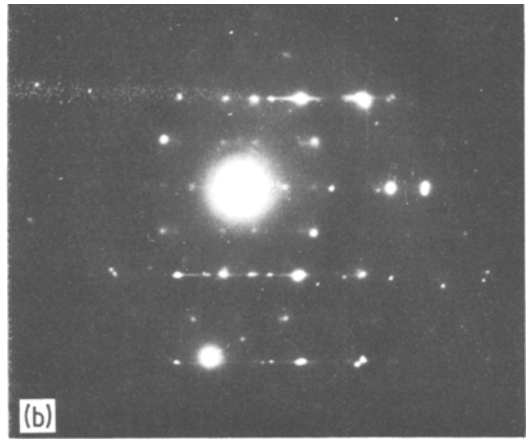

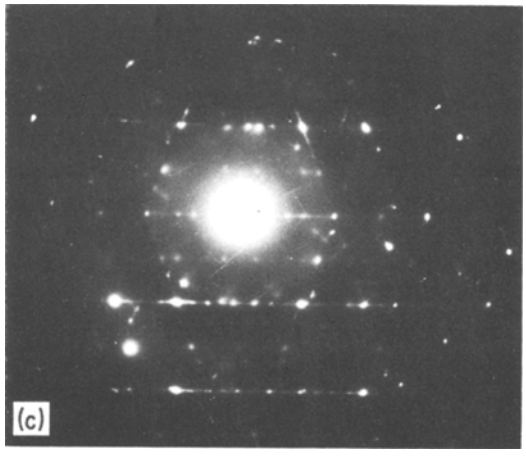

Figure 17 Diffraction patterns showing the destruction of long-range order (as revealed by streaking) when the foils are heat treated at 853 K for 30 ksec.

4.3. The $Al_{13}Rh_4$ intermediate phase

The intermediate phase formed after decomposition of the supersaturated solid solution has been found to have a monoclinic structure, whose lattice parameters are quite different from those of the Al_9Rh_2 phase. Since metastable crystalline phases form during decomposition of supersaturated solid solutions (both in solid-state quenched and melt-quenched cases), it is possible that this is a metastable phase. Continued annealing at higher temperatures and for long times has not changed the crystal structure of this phase, although the size and shape of the precipitates have changed. Even on heating the alloy to almost the melting point, the constitution does not change and thus, we can consider this an equilibrium phase. Reasons for assigning this particular chemical formula for this phase have been elaborated in an earlier paper [13].

A question – whether Al_9Rh_2 also is an equilibrium phase – was posed and left unanswered in our earlier paper [13]. Since the alloy under investigation contains only 2 wt% Rh, the equilibrium constitution should be the aluminium solid solution and the most aluminium-rich Al–Rh intermediate phase. If Al_9Rh_2 also is an equilibrium phase, one should have obtained a mixture of aluminium solid solution and Al_9Rh_2 at least on heating the alloy almost up to the melting point and cooling it down to room temperature. Our results, on the other hand, indicate that we obtain only $Al_{13}Rh_4$ and not Al_9Rh_2 which clinches the issue and suggests that perhaps the composition and/or lattice parameters assigned to Al_9Rh_2 [28] are wrong.

5. Conclusions

The present investigation brings out the following interesting conclusions:

1. The solid solubility of rhodium in aluminium can be increased by melt quenching at least up to 2 wt%.

2. The metastable supersaturated solid solution is quite stable up to 643 K on continuous heating and on further heating precipitates an intermediate phase.

3. The precipitate phase was found to have a needle or bulk shape. When present as needles, this phase forms the classical Widmanstätten pattern.

4. The intermediate phase has been found to have a monoclinic structure with $a = 1.636$ nm, $b = 0.805$ nm, $c = 1.279$ nm and $\beta = 107.77°$. This is an equilibrium phase.

5. Very long annealing treatments at relatively higher temperatures of 773 K resulted in the

formation of an ordered phase. The long-range order was destroyed on heating the alloys further.

6. Rapid cooling from near the melting point resulted in the formation of a lamellar structure.

Acknowledgements

The authors are indebted to Professor T. R. Anantharaman for encouragement and to the Head of the Department of Metallurgical Engineering, B.H.U., for provision of laboratory facilities. They are also grateful to Dr G. V. S. Sastry for a critical reading of the manuscript.

References

1. P. DUWEZ, *Trans. ASM Qly.* **60** (1967) 607.
2. T. R. ANANTHARAMAN and C. SURYANARAYANA, *J. Mater. Sci.* **6** (1971) 1111.
3. H. JONES and C. SURYANARAYANA, *ibid.* 8 (1973) 705.
4. T. R. ANANTHARAMAN, P. RAMACHANDRARAO, C. SURYANARAYANA, S. LELE and K. CHATTOPADHYAY, *Trans. Indian Inst. Met.* **30** (1977) 423.
5. C. SURYANARAYANA, "Rapidly Quenched Metals – A Bibliography 1973–1979" (IFI/Plenum, New York, 1980).
6. H. JONES, "Rapid Solidification of Metals and Alloys", Monograph No. 8 (Institution of Metallurgists, London, 1982).
7. G. V. S. SASTRY and C. SURYANARAYANA, *Mater. Sci. Eng.* **47** (1981) 193.
8. G. V. S. SASTRY, C. SURYANARAYANA and G. VAN TENDELOO, *Phys. Status Solidi (a)* **73** (1982) 267.
9. Z. A. CHAUDHURY, G. V. S. SASTRY and C. SURYANARAYANA, *Z. Metallkd.* **73** (1982) 201.
10. Z. A. CHAUDHURY and C. SURYANARAYANA, *J. Mater. Sci.* **17** (1982) 3158.
11. *Idem, Philips Electron Opt. Bull.* **118** (1982) 23.
12. *Idem, Thin Solid Films* **98** (1982) 233.
13. *Idem, J. Less-Common Met.* **91** (1983) 181.
14. F. A. SHUNK, "Constitution of Binary Alloys", Second Supplement (McGraw-Hill, New York, 1969) p. 40.
15. L. F. MONDOLFO, "Aluminium Alloys, Structure and Properties" (Butterworths, London, 1976).
16. W. B. PEARSON, "A Handbook of Lattice Spacings and Structures of Metals and Alloys", Vol. 2 (Pergamon Press, Oxford, 1967).
17. P. DUWEZ and R. H. WILLENS, *Trans. TMS-AIME* **227** (1963) 362.
18. D. B. WILLIAMS and J. W. EDINGTON, in "Rapidly Quenched Metals" (Proceedings of the 2nd International Conference), edited by N. J. Grant and B. C. Giessen, (M.I.T. Press, Cambridge, 1976) p. 135.
19. H. JONES, in "Vacancies '76", edited by R. E. Smallman and J. E. Harrier (The Metals Society, London, 1977) p. 175.
20. L. R. K. RAO, C. SURYANARAYANA and S. LELE, *Aluminium* **58** (1982) 214.
21. P. H. SHINGU, J. TAKAMURA and M. KAWASHIMA, *Suiyokwai-Shi* **16** (1968) 472 (in Japanese).
22. *Idem, Met. Abs. Light Met. Alloys Jpn.* 4 (1969) 101.
23. G. V. S. SASTRY, C. SURYANARAYANA, G. VAN TENDELOO and M. VAN SANDE, *Mater. Res. Bull.* **13** (1978) 1065.
24. P. FURRER, T. R. ANANTHARAMAN and H. WARLIMONT, *Phil. Mag.* **21** (1970) 873.
25. P. DUWEZ, R. H. WILLENS and W. KLEMENT, *J. Appl. Phys.* **31** (1960) 1136.
26. G. SRIDHAR, M. HANUMANTHA RAO and C. SURYANARAYANA, unpublished results (1982).
27. B. C. GIESSEN and R. H. WILLENS, "Phase Diagrams: Materials Science and Technology" Vol. 3, edited by A. M. Alper (Academic Press, New York, 1970) p. 103.
28. L. EDSHAMMAR, *Acta Chem. Scand.* **22** (1968) 2822.

Received 6 December 1982
and accepted 18 February 1983